

# The critical parameters in in-situ MgB<sub>2</sub> wires and tapes with ex-situ MgB<sub>2</sub> barrier after hot isostatic pressure, cold drawing, cold rolling and doping

D. Gajda, A. Morawski, A. J. Zaleski, W. Häßler, K. Nenkov, M. A. Rindfleisch, E. Żuchowska, G. Gajda, T. Czujko, T. Cetner, and M. S. A. Hossain

Citation: *Journal of Applied Physics* **117**, 173908 (2015); doi: 10.1063/1.4919364

View online: <https://doi.org/10.1063/1.4919364>

View Table of Contents: <http://aip.scitation.org/toc/jap/117/17>

Published by the [American Institute of Physics](#)

---

## Articles you may be interested in

[Experimental research of high field pinning centers in 2% C doped MgB<sub>2</sub> wires at 20 K and 25 K](#)

*Journal of Applied Physics* **120**, 113901 (2016); 10.1063/1.4962399

[Enhanced higher temperature \(20–30 K\) transport properties and irreversibility field in nano-Dy<sub>2</sub>O<sub>3</sub> doped advanced internal Mg infiltration processed MgB<sub>2</sub> composites](#)

*Applied Physics Letters* **105**, 112603 (2014); 10.1063/1.4896259

[Universal relationship between crystallinity and irreversibility field of MgB<sub>2</sub>](#)

*Applied Physics Letters* **86**, 212502 (2005); 10.1063/1.1937991

[A defect detection method for MgB<sub>2</sub> superconducting and iron-based Ba\(Fe,Co\)<sub>2</sub>As<sub>2</sub> wires](#)

*Applied Physics Letters* **108**, 152601 (2016); 10.1063/1.4947056

[Al-doped MgB<sub>2</sub> materials studied using electron paramagnetic resonance and Raman spectroscopy](#)

*Applied Physics Letters* **108**, 202601 (2016); 10.1063/1.4949338

[High critical current density and improved irreversibility field in bulk MgB<sub>2</sub> made by a scaleable, nanoparticle addition route](#)

*Applied Physics Letters* **81**, 2026 (2002); 10.1063/1.1506184

---

**AIP** | Journal of Applied Physics SPECIAL TOPICS



# The critical parameters in *in-situ* MgB<sub>2</sub> wires and tapes with *ex-situ* MgB<sub>2</sub> barrier after hot isostatic pressure, cold drawing, cold rolling and doping

D. Gajda,<sup>1,a)</sup> A. Morawski,<sup>2</sup> A. J. Zaleski,<sup>3</sup> W. Häbler,<sup>4</sup> K. Nenkov,<sup>1,4</sup> M. A. Rindfleisch,<sup>5</sup> E. Zuchowska,<sup>6</sup> G. Gajda,<sup>1</sup> T. Czujko,<sup>6</sup> T. Cetner,<sup>2</sup> and M. S. A. Hossain<sup>7</sup>

<sup>1</sup>International Laboratory of HMF and LT, Gajowicka 95, 53-421 Wrocław, Poland

<sup>2</sup>Institute of High Pressure Physics PAS, Sokolowska 29/37, 01-142 Warsaw, Poland

<sup>3</sup>Institute of Low Temperature and Structure Research PAS, Okólna 2, 50-422 Wrocław, Poland

<sup>4</sup>Institute for Solid State and Materials Research Dresden, P.O. Box 270016, D-01171 Dresden, Germany

<sup>5</sup>Hyper Tech Research, Inc., 1275 Kinnear Road, Columbus, Ohio 43212, USA

<sup>6</sup>Military Technical Academy, ul. gen. Sylwester Kaliski 2, 00-908 Warsaw, Poland

<sup>7</sup>Institute for Superconducting and Electronic Materials, AIIM, University of Wollongong, North Wollongong, NSW-2519, Australia

(Received 16 January 2015; accepted 13 March 2015; published online 5 May 2015)

MgB<sub>2</sub> precursor wires were prepared using powder in tube technique by Institute of High Pressure PAS in Warsaw. All samples were annealed under isostatic pressure generated by liquid Argon in the range from 0.3 GPa to 1 GPa. In this paper, we show the effects of different processing routes, namely, cold drawing (CD), cold rolling (CR), hot isostatic pressure (HIP) and doping on critical current density ( $J_c$ ), pinning force ( $F_p$ ), irreversible magnetic-field ( $B_{irr}$ ), critical temperature ( $T_c$ ),  $n$  value, and dominant pinning mechanism in MgB<sub>2</sub>/Fe wires with *ex situ* MgB<sub>2</sub> barrier. The results show that medium pressures ( $\sim 0.35$  GPa) lead to high  $J_c$  in low and medium magnetic fields (0 T – 9 T). On the other hand, higher pressures ( $\sim 1$  GPa) lead to enhanced  $J_c$  in high magnetic fields (above 9 T). Transport measurements show that CD, CR, and HIP have small effects on  $B_{irr}$  and  $T_c$ , but CD, CR, HIP, and doping enhance  $J_c$  and  $F_p$  in *in situ* MgB<sub>2</sub> wires with *ex situ* MgB<sub>2</sub> barrier. Transport measurements on *in situ* undoped MgB<sub>2</sub> wire with *ex situ* MgB<sub>2</sub> barrier yield a  $J_c$  of about 100 A/mm<sup>2</sup> at 4.2 K in 6 T, at 10 K in 4 T and at 20 K in 2 T. The results also show that cold drawing causes increase of  $n$  value. © 2015 AIP Publishing LLC.

[<http://dx.doi.org/10.1063/1.4919364>]

## I. INTRODUCTION

MgB<sub>2</sub> as a superconducting material was discovered in 2001.<sup>1</sup> Pure (undoped) MgB<sub>2</sub> wires have relatively high critical temperature, low anisotropy, low critical current density ( $J_c$ ) in high magnetic fields, and low irreversible magnetic field ( $B_{irr}$ ). The studies show that  $J_c$  and  $B_{irr}$  in MgB<sub>2</sub> wires with Nb, Ti, and Ta barrier can be increased by improvement of the MgB<sub>2</sub> precursor material density and the creation of pinning centers. Processes such as hot isostatic pressure (HIP), cold drawing (CD), cold rolling (CR), cold pressure (CP), and doping all have been shown to improve these properties. Precursor powders of high purity are desired because impurities reduce the density and uniformity of the MgB<sub>2</sub> material. The high density of MgB<sub>2</sub> material is very important because it allows for large number of connections between the grains.

HIP process increases density and homogeneity of MgB<sub>2</sub> materials, number of connections between grains, and dislocation density while it reduces the size of voids.<sup>2,3</sup> Gajda *et al.*<sup>4</sup> showed that MgB<sub>2</sub> material annealed under a 0.1 MPa Argon pressure has larger grain size than that of MgB<sub>2</sub> material annealed at 1 GPa. These results indicate that HIP process influences grain size. Adamczyk *et al.*<sup>5</sup> showed HIP-processed SiC doped MgB<sub>2</sub> wires with Nb barrier

having a critical current density of 100 A/mm<sup>2</sup> at 4.2 K in magnetic field of 14 T.

The results in these articles<sup>6–8</sup> indicate that cold rolling improves homogeneity of MgB<sub>2</sub> material. Hancock *et al.*<sup>6</sup> showed that CR increases *in situ* MgB<sub>2</sub> material density of about 37% and *ex situ* MgB<sub>2</sub> material density of about 19%. Higher density of MgB<sub>2</sub> material leads to more connections between grains. Moreover, the results presented by Häbler *et al.*<sup>8</sup> showed a CR-processed wire attaining a critical current density of 100 A/mm<sup>2</sup> at 4.2 K in magnetic field of 16.4 T.

The studies by Uchiyama *et al.*<sup>9</sup> and Susner *et al.*<sup>10</sup> indicate that CD leads to increased homogeneity of MgB<sub>2</sub> material, larger length and outer surface of Mg grains, reduced thickness of Mg grains, and improved critical current density ( $J_c$ ) in MgB<sub>2</sub> wires. Susner *et al.* obtained a critical current density of 100 A/mm<sup>2</sup> at 4.2 K in magnetic field of 12 T in MgB<sub>2</sub> wires with Nb barrier.<sup>10</sup>

Published results also suggest that doping of SiC and C leads to increase in  $J_c$  and  $B_{irr}$ ,<sup>8,11,12</sup> and can accelerate formation of superconducting phase.<sup>13,14</sup>

Research presented by Häbler *et al.*<sup>8</sup> shows that the process of mechanical alloying can increase the density of the MgB<sub>2</sub> material. This technology allows to obtain 100 A/mm<sup>2</sup> at 12 T and 4.2 K in the undoped MgB<sub>2</sub> tape.

CP also can increase critical parameters and homogeneity of MgB<sub>2</sub> wires with Nb barrier. Pressure of 1.48 GPa in

<sup>a)</sup>E-mail: gajda@ml.pan.wroc.pl, dangajda@op.pl

doped *in situ* MgB<sub>2</sub> material leads to  $J_c$  of 100 A/mm<sup>2</sup> at 4.2 K in magnetic field of 13 T.<sup>15</sup> In pure *in situ* MgB<sub>2</sub>, a pressure of 1.5 GPa produces a  $J_c$  of 100 A/mm<sup>2</sup> at 4.2 K in magnetic field of 9 T,<sup>16</sup> whereas pressure of 1.5 GPa leads to a  $J_c$  of 100 A/mm<sup>2</sup> at 4.2 K in magnetic field of 5.7 T in *ex situ* MgB<sub>2</sub> material.<sup>17</sup>

Currently, *in situ* MgB<sub>2</sub> wires are fabricated by two methods: with barriers<sup>16,18,19</sup> and without barriers.<sup>20–22</sup> Metal barriers are made with Nb, Ta, and Ti.<sup>16,18,19</sup> *In situ* MgB<sub>2</sub> wires with barriers have high  $J_c$ ,  $B_{irr}$ , and  $B_{c2}$ . However, metal barriers can break during cold working (CD, CR, CP). Each defect in the barrier may reduce  $J_c$  in MgB<sub>2</sub> wire. *In situ* MgB<sub>2</sub> wires without barriers have low  $J_c$  in the medium and high magnetic fields,<sup>20</sup> because metallic phases such as: Fe<sub>2</sub>B,<sup>8</sup> CuMg<sub>2</sub>,<sup>20</sup> and Cu<sub>2</sub>Mg<sup>20</sup> are created during reaction. The metallic phases decrease the amount of superconducting material.

Recently, a new diffusion barrier with an *ex situ* MgB<sub>2</sub> material was studied. This concept was previously showed by Morawski *et al.* from Institute of High Pressure Physics PAS.<sup>23</sup> Current studies indicate that MgB<sub>2</sub> wires with an *ex situ* MgB<sub>2</sub> barrier have lower  $J_c$  anisotropy (i.e., small difference between the  $J_c$  in the perpendicular and parallel magnetic fields), higher homogeneity, and allows to obtain pure *in situ* MgB<sub>2</sub> material.<sup>24–26</sup>

In this article, we present the effects of HIP, CD, CR, and C—additives on  $J_c$ ,  $B_{irr}$ , and  $T_c$  in MgB<sub>2</sub> wires made with an *ex situ* MgB<sub>2</sub> barrier.

## II. EXPERIMENTAL

### A. Wires preparation

Monofilament MgB<sub>2</sub> wires with an *ex situ* MgB<sub>2</sub> barrier were fabricated at the Institute of High Pressure PAS in Warsaw. Figure 1 shows a cross sectional and longitudinal sectional of MgB<sub>2</sub> wire with *ex situ* MgB<sub>2</sub> barrier. These wires have been produced by modified Powder in Tube (PIT) method using multi cold isostatic pressure (CIP). *In situ* MgB<sub>2</sub> precursor materials were made from commercial powders of Mg (99.8% purity), MgH<sub>2</sub> powders from ABCR GmbH Karlsruhe, amorphous boron powder (University of Geneva), and carbon from Institute for Solid State and Materials Research Dresden. The *in situ* MgB<sub>2</sub> precursor materials were milled for 48 h and then CIP-ed (at the pressure of 0.3 GPa) to form rods of ca 8 mm diameters.<sup>25,27</sup> Then the *ex situ* MgB<sub>2</sub> powders (Alfa Aesar) prepared with

or without additives were milled for 4 h and ultrasonically cleaned and then were used to fill around the rods. The assembly of these precursor billets of *in situ* MgB<sub>2</sub> rods with surrounding *ex situ* MgB<sub>2</sub> powder in an Fe tube took place inside a He gas atmosphere glove box.<sup>25,27</sup>

These *in situ* MgB<sub>2</sub> rods with surrounding *ex situ* MgB<sub>2</sub> powder in an Fe tube were cold drawing to 1.8 mm and 1.6 mm diameter. Sample Nos. 2 and 3 were obtained by using cold drawing with sample No 1. MgB<sub>2</sub> tapes were obtained by cold rolling the same precursor billets. All the wires and tapes after cold drawing were annealed under isostatic pressure (argon) in range from 0.3 GPa to 1 GPa. (Table I—doping level—at. %). The *Ex situ* MgB<sub>2</sub> barrier makes up about 15% of total MgB<sub>2</sub> material (*in situ* MgB<sub>2</sub> and *ex situ* MgB<sub>2</sub>) which itself is 35% of the wire.

### B. The measurements' conditions

The critical current ( $I_c$ ) of the wires was measured by the four-probe resistive method in a liquid helium bath inside the Bitter type magnet of 25 mm diameter at International Laboratory of HMF & LT in Wroclaw. A well stabilized magnetic field was generated by the Bitter type magnet operating up to ~14 T. A constant current source was the gain current (maximum 150 A).<sup>4,26</sup> Transport critical current measurements were performed at 10 K, 20 K, and 25 K at the Institute for Solid State and Materials Research in Dresden.<sup>8</sup> The 1  $\mu$ V/cm criterion was used for  $I_c$  evaluation.

The samples in perpendicular magnetic field were of 20 mm length and in parallel magnetic field were of 70 mm length. The critical temperature was measured using four-probe resistive method using AC current (5 mA, 14 Hz) at International Laboratory of HMF & LT by using PPMS Model 7100 (Quantum Design—in the field ranging from 0 up to 14 T).

Analysis of the microstructure was performed with Quanta 3D FEG Dual Beam at Military Technical Academy in Warsaw and by Zeiss microscope (high resolution low-energy type) at the Institute of High Pressure Physics PAS in Warsaw.

## III. RESULTS

### A. SEM analysis

*Ex situ* MgB<sub>2</sub> barrier creates very good connectivity with iron shield, because—between *ex situ* MgB<sub>2</sub> barrier and metal shields—voids and cracks did not appear (Figs. 1(a) and 1(b)).

*Ex situ* MgB<sub>2</sub> barrier makes very good contact with undoped *in situ* MgB<sub>2</sub> material (Figs. 1(a) and 1(b)), because—between *ex situ* MgB<sub>2</sub> barrier and *in-situ* MgB<sub>2</sub>—cracks and voids are not formed. SEM results show that in microstructure of the *ex situ* MgB<sub>2</sub> barriers and *in situ* MgB<sub>2</sub>, material cracks are not formed (Fig. 1).

The results on Figure 2 for MgB<sub>2</sub> wire with *ex situ* MgB<sub>2</sub> barrier show that cold drawing significantly reduces size of the defects and increases homogeneity of the MgB<sub>2</sub> material. The appearance in the sample 3 of layer structure (Fig. 2(d)) invisible in the sample 2 suggests that Mg in

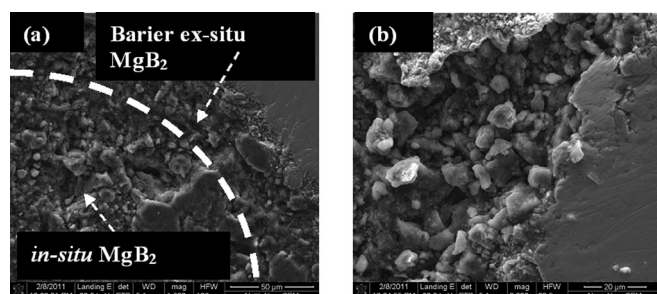


FIG. 1. The secondary electron view of the cross section (a) and (b) for sample 1.

TABLE I. HIP-ing parameters of various samples. Fe–iron sheath.

Samples identifier	Wire diameter (mm)	<i>In situ</i> material	<i>Ex-situ</i> barrier	Pressure (GPa)	Sintering temperature (°C)	Sintering time (min)
1	Fe	Mg + 2B	<i>ex situ</i>	1	750	40
	1.6		MgB <sub>2</sub>			
2	Fe	Mg + 2B	<i>ex situ</i>	1	750	40
	1.1		MgB <sub>2</sub>			
3	Fe	Mg + 2B	<i>ex situ</i>	1	750	40
	0.75		MgB <sub>2</sub>			
4	Fe	Mg + 2B	<i>ex situ</i>	0.35	750	40
	1.6		MgB <sub>2</sub>			
5	Fe	MgH <sub>2</sub> + 2B	<i>ex situ</i>	1	750	40
	1.6		MgB <sub>2</sub>			
6	Fe	MgH <sub>2</sub> + 2B	<i>ex situ</i>	1	750	40
	0.6 × 2.5		MgB <sub>2</sub>			
7	Fe	Mg + 5%Mg + 2B	<i>ex situ</i>	0.3	700	10
	1.8		MgB <sub>2</sub>			
8	Fe	Mg + 5%Mg + 2B + 6%C	<i>ex situ</i>	0.3	700	10
	1.8		MgB <sub>2</sub> + 6% C			

MgB<sub>2</sub> wire with the *ex situ* MgB<sub>2</sub> barrier during cold drawing increases the length just like Mg in MgB<sub>2</sub> wires with Fe and Nb barrier.

The results on Fig. 3 for MgB<sub>2</sub> wires with *ex situ* MgB<sub>2</sub> barrier show that increase of pressure from 0.3 GPa to 1 GPa allows to obtain smaller grains and voids and higher density MgB<sub>2</sub> material. Smaller grains allow to obtain more connections between grains. Similar results obtained Morawski *et al.*<sup>27</sup> and Cetner *et al.*<sup>28</sup> for MgB<sub>2</sub> wires with Nb barrier. They indicate that annealing in a pressure of 1 GPa leads to grain size of about 50 nm.

SEM results on Figs. 4(a) and 4(b) show that the *ex situ* MgB<sub>2</sub> barrier creates good connection with iron sheath after rolling and HIP, because between iron sheath and *ex situ*

MgB<sub>2</sub> barrier are not formed cracks. We see on Fig. 4(a) that the *ex situ* MgB<sub>2</sub> barrier creates good connection of *in situ* MgB<sub>2</sub>, because—between the *in situ* MgB<sub>2</sub>, and *ex situ* MgB<sub>2</sub> barrier—cracks are not formed. Moreover, SEM results show that cold rolling and annealing in high pressure increases the density of the MgB<sub>2</sub> material in wires with *ex situ* MgB<sub>2</sub> barrier. Above mentioned results suggest that the *ex situ* MgB<sub>2</sub> barrier can be used in production of MgB<sub>2</sub> tapes because rolling does not cause damage to the microstructure of MgB<sub>2</sub> tapes.

EDX and XRD studies presented by Kario *et al.*<sup>24</sup> showed that the *ex situ* MgB<sub>2</sub> barrier allows to obtain high-purity *in situ* MgB<sub>2</sub> material.

## B. MgB<sub>2</sub> wires with *ex situ* MgB<sub>2</sub> barrier in an iron sheath (at 4.2 K)

Figure 5(a) shows the effects of pressure and wires diameter on critical current density ( $J_c$ ). These results indicate that annealing in a pressure of 0.35 GPa leads to a significant increase in critical current density in low and medium magnetic fields (from 0 T to 9 T) in comparison with sample 1 (1 GPa). However, annealing in a pressure of 1 GPa leads to an increase in  $J_c$  in magnetic field above 9 T over that of sample 4 (0.35 GPa). Measurements and calculations show that reduction (CD) of the diameter from 1.6 mm to 1.1 mm and the surface (cross section of filament) of MgB<sub>2</sub> wire

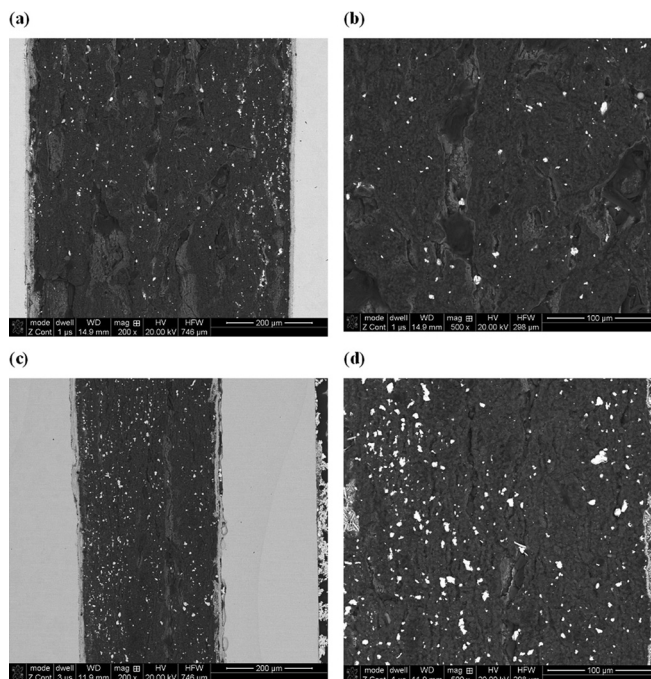


FIG. 2. The secondary electron analysis—longitudinal section: (a) and (b) sample 2; (c) and (d) sample 3.

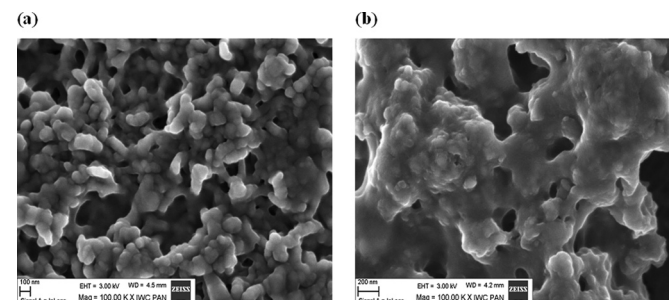


FIG. 3. The secondary electron analysis—cross section: (a) sample 1 and (b) sample 4.

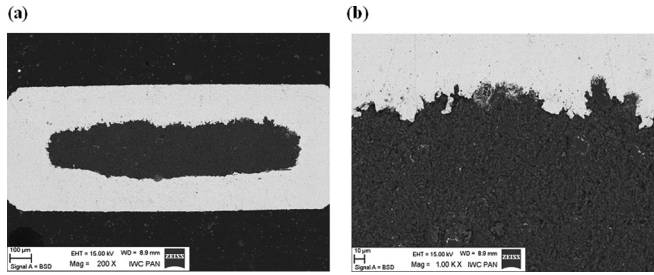


FIG. 4. The secondary electron view—cross section: (a) and (b) sample 6.

with *ex situ* MgB<sub>2</sub> barrier by about 52% leads to a significant increase in  $J_c$  in magnetic fields from 0 T to 12 T. A further reduction of diameter from 1.1 mm to 0.75 mm and surface (cross section of filament) of MgB<sub>2</sub> wire with *ex situ* MgB<sub>2</sub> barrier of about 55% leads to an additional increase in  $J_c$  in magnetic fields from 0 T to 12 T. The Kramer analysis was done with formula  $J_c^{0.5} * B^{0.25}$ .<sup>29</sup> This analysis determines irreversible magnetic field ( $B_{irrK}$ ). Figure 5(b) shows that annealing in high pressure might increase  $B_{irrK}$  (about 4.8%) and cold drawing does not increase  $B_{irrK}$ . Figure 5(c) indicates that annealing in a pressure of 0.35 GPa increases density of pinning centers in low and medium magnetic fields.

These results suggest that medium pressure significantly increases density of surface (big voids)<sup>30</sup> and point pinning centers (voids similar in size to the coherence length).<sup>30</sup> However, annealing in a pressure of 1 GPa leads to an increase in the density of pinning centers in high magnetic fields.<sup>2</sup> These results suggest that high pressure increases density of line pinning centers.<sup>30</sup> Figure 5(d) shows the effects of pressure and wires diameter on reduced  $F_p/F_{pmax}$  as a function of reduced  $B/B_{irrK}$ . These results suggest that cold drawing and pressure do not change dominant pinning mechanism in undoped MgB<sub>2</sub> wires (surface pinning centers). The results in Figs. 5(a) and 5(e) showed that difference in  $J_c$  in the perpendicular and parallel direction of the magnetic field (a measure of  $J_c$  anisotropy) in the wires of 1.6 mm, 1.1 mm, and 0.75 mm diameter after annealing in a pressure of 1 GPa is about 4%–7% (Fig. 5(e)). On the other hand, for the MgB<sub>2</sub> wires annealed for a pressure of 0.35 GPa, the anisotropy is about 14% (Fig. 5(e)).

Figure 6 shows the effects of cold rolling and the use of MgH<sub>2</sub> powder in place of pure Mg on  $J_c$  and  $F_p$ . These results indicate that MgH<sub>2</sub> powder can increase  $J_c$  and  $F_p$  in low and medium magnetic fields (from 0 T to 7 T) compared to the sample made with pure Mg powder. We can see that

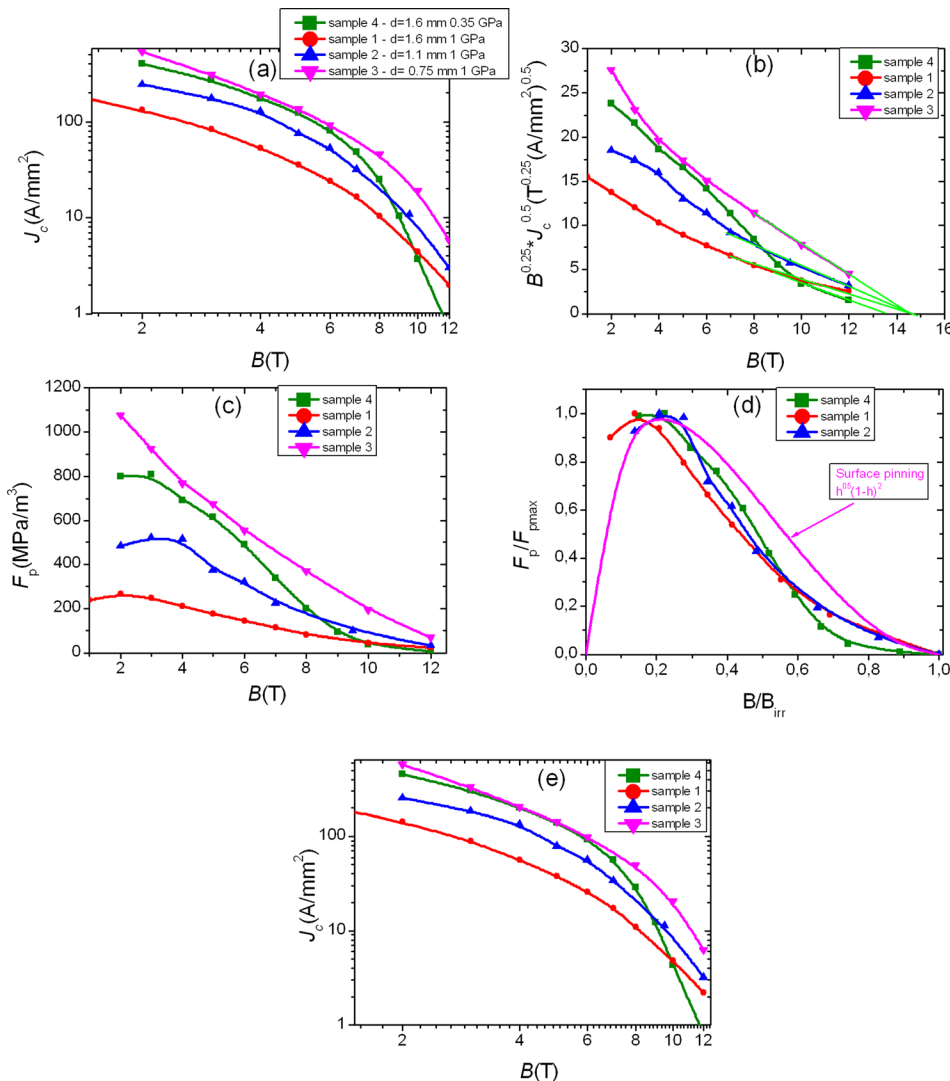


FIG. 5. (a) The critical current density as function of perpendicular magnetic field,  $J_c = f(B)$ . (b) The variation of  $B^{0.25} J_c^{0.5}$  with perpendicular magnetic field. (c) The pinning force as function of perpendicular magnetic field,  $F_p = f(B)$ . (d) The reduced pinning force as a function of reduced perpendicular magnetic field,  $F_p/F_{pmax} = f(h)$ . (e) The critical current density as function of parallel magnetic field,  $J_c = f(B)$ .  $F_{pmax}$  means maximum pinning.

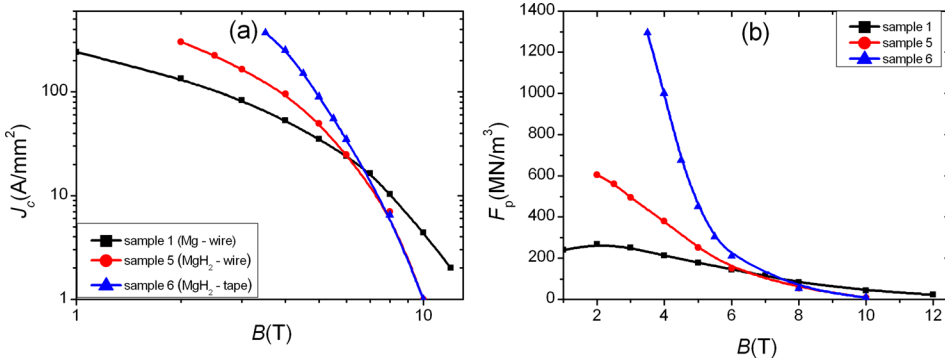


FIG. 6. (a) The critical current density as function of magnetic field,  $J_c = f(B)$ . (b) The pinning force as function of magnetic field,  $F_p = f(B)$ . The measurements were made in perpendicular magnetic field for samples 1, 5, and 6 at 4.2 K.

pure Mg powder is associated with higher critical current density and more pinning centers in MgB<sub>2</sub> wires with *ex situ* MgB<sub>2</sub> barrier in high magnetic fields ( $>7$  T). The Kramer analysis indicates that the MgH<sub>2</sub> powder reduced  $B_{irrK}$  by 20%, compared to samples obtained with pure Mg powder. Fig. 6(b) shows that MgH<sub>2</sub> powder can increase the density of surface and point pinning centers and reduce the density of line pinning centers. Results for samples 5 and 6 with MgH<sub>2</sub> powder show that cold rolling increases  $J_c$  and  $F_p$  in low and medium magnetic fields (from 0 to 7 T) and does not change  $J_c$  and  $F_p$  in high magnetic fields. These results show that cold rolling increases density of surface and point pinning centers (Fig. 6(b)). It also indicates that cold rolling does not increase the density of line pinning centers in MgB<sub>2</sub> tape. The Kramer analysis shows that cold rolling does not increase  $B_{irrK}$  (of about 11.5 T).

Figure 7(a) shows the effect of C doping on  $J_c$  as a function of magnetic field. These results indicate that the C dopant poorly increases  $J_c$  in magnetic fields from 4 T to 8 T. Moreover, we see that C dopant significantly increases  $J_c$  in magnetic fields above 8 T. However, results show that C dopant does not increase  $J_c$  in magnetic fields from 0 T to

4 T. Fig. 7(b) indicates that the C dopant increases  $B_{irrK}$  by about 1.5 T (10%—in sample 6). This dopant shifts  $F_{pmax}$  to higher magnetic fields (3 T) and increases density of pinning centers from 4 T to 14 T. Fig. 7(c) suggests that C dopant creates point and line pinning centers and does not form surface pinning centers.<sup>30</sup> Comparing results of samples 7 and 8 (Fig. 7(d)), we can see that C dopant does not change the dominant pinning mechanism. This dominant pinning mechanism is characteristic for pure MgB<sub>2</sub> material. These results might suggest that the 6% C dopant is too small to change the dominant pinning mechanism.

### C. Measurements in 10 K, 20 K, and 25 K

The results in Fig. 8(a) show that the reduction in diameter of wires from 1.1 mm to 0.75 mm leads to an increase in  $J_c$  at 10 K by about 35%, at 20 K by about 50%, and at 25 K by about 15%. Increase of temperature from 4.2 K to 25 K leads to decrease in  $J_c$  in all magnetic fields. The Kramer analysis (Fig. 8(b)) suggests that cold drawing does not change the value of  $B_{irr}$  (10 K -  $B_{irrK} = 10.3$  T, 20 K -  $B_{irrK} = 6.3$  T, 25 K -  $B_{irrK} = 3$  T). Increase in temperature

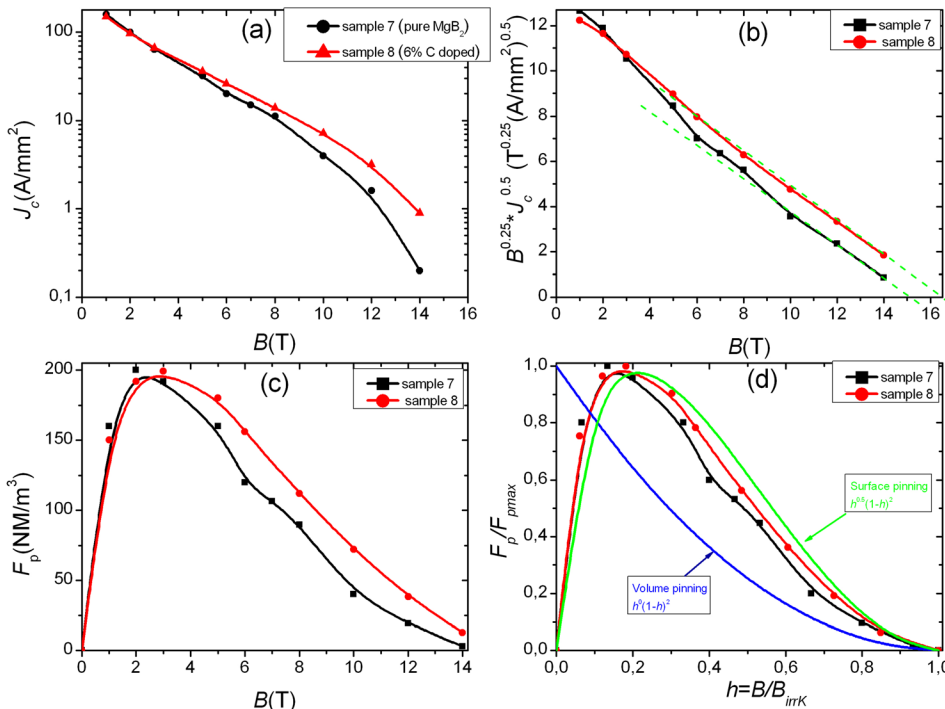


FIG. 7. (a) The critical current density as function of magnetic field,  $J_c = f(B)$ . (b) The variation of  $B^{0.25}J_c^{0.5}$  with magnetic field. (c) The pinning force as function of magnetic field,  $F_p = f(B)$ . (d) The reduced pinning force as a function of reduced magnetic field,  $F_p/F_{pmax} = f(h)$ . The measurements were made in perpendicular magnetic field for samples 7 and 8 at 4.2 K. The green line determines the irreversible magnetic field ( $B_{irr}$ ) on Figure 7(b).

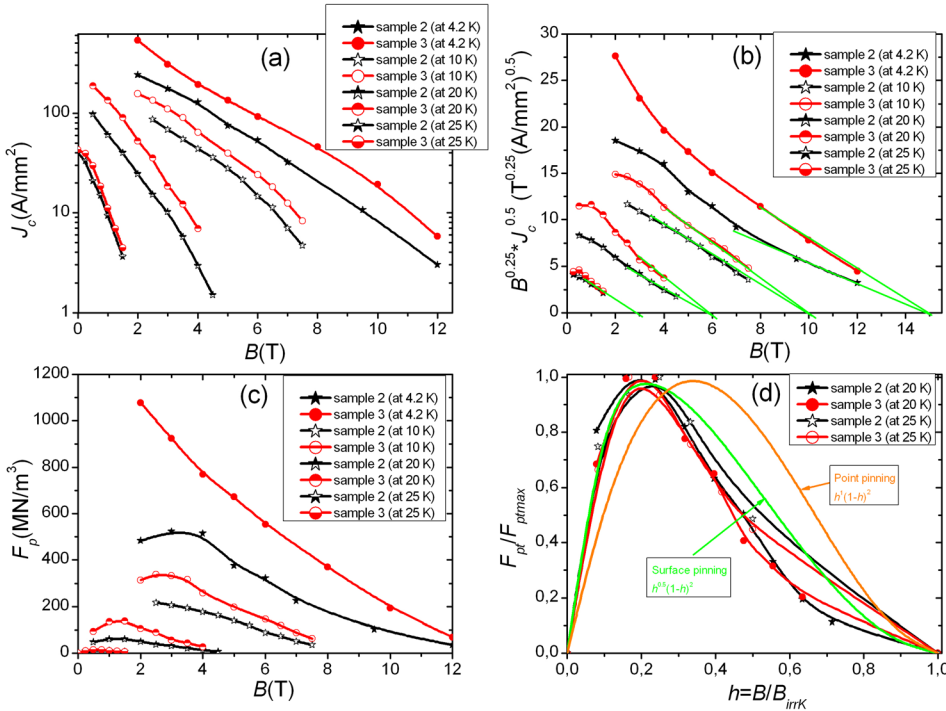


FIG. 8. (a) The critical current density as function of magnetic field,  $J_c = f(B)$ . (b) The variation of  $B^{0.25} J_c^{0.5}$  with magnetic field. (c) The pinning force as function of magnetic field,  $F_p = f(B)$ . (d) The reduced pinning force as a function of reduced magnetic field,  $F_p/F_{pmax} = f(h)$ . The measurements were made in perpendicular magnetic field for samples 2 and 3. The green line determines the irreversible magnetic field ( $B_{irr}$ ) on Figure 8(b).

from 4.2 K to 25 K leads to a decrease in  $B_{irrK}$  by about 40%. The calculations of transport pinning force (Fig. 8(c)) indicate that cold drawing significantly increases pinning centers density in low magnetic fields (at 10 K and 20 K). These results suggest that cold drawing slightly increases  $F_p$  in high magnetic fields. Figure 8(a) shows that cold drawing did not lead to an increase in  $J_c$  at 25 K. Results of scaling show that cold drawing does not change dominant pinning mechanism in pure MgB<sub>2</sub> wires made with an *ex situ* MgB<sub>2</sub> barrier. Figure 8(d) indicates that dominant pinning mechanism is provided by surface pinning centers.

#### D. $T_c$ and $B_{irr}$

The results in Fig. 9(a) show that cold drawing does not change critical temperature ( $T_c$ ).  $T_c$  is about 37.5 K. Figure 9(a) indicates that the 1 GPa pressure improves connection between grains in undoped MgB<sub>2</sub> wires of smaller diameter, because resistance in normal state of sample 3 is lower than that of sample 2 by about 22%.  $B_{irr}$  with resistance measurements was determined on the basis of 5% ( $B_{irrR}$ ).<sup>29</sup> The value of  $B_{irrR}$  does not change after cold drawing (Fig. 9(b)). When comparing results of  $B_{irr}$  from the Kramer analysis ( $B_{irrK}$ )

(Fig. 5(b)) with results  $B_{irrR}$  (Fig. 9(b)), we see that  $B_{irrK}$  is lower than  $B_{irrR}$  by about 8%. This result suggests that the Kramer analysis provides an acceptable estimate of the value of  $B_{irr}$  in undoped MgB<sub>2</sub> wires with *ex situ* MgB<sub>2</sub> barrier.

In Fig. 10(a), we see that annealing under 1 GPa pressure (sample 1) slightly decreases  $T_c$  in comparison with sample after annealing under 0.35 GPa pressure (sample 4). Figure 10(a) shows that the annealing under high pressure improves connection between grains in undoped MgB<sub>2</sub> better than annealing under medium pressure, because resistance in normal state of sample 1 is lower than that of sample 4 by about 10%. In Fig. 10(b), we see that annealing under 1 GPa pressure slightly decreases  $B_{irr}$  at temperature above 22.5 K and slightly increases  $B_{irr}$  at temperature below 22.5 K.

#### E. $n$ value

The coefficient of  $n$  value was determined from the formula  $(E/E_c) = \alpha(I/I_c)^n$ .<sup>31</sup> Ghosh<sup>31</sup> shows that the  $n$  value depends on internal factors (connectivity between the grains, pinning centers, and flux creep) and external factors (distribution and quality of the filaments). The  $n$  value is also dependent on homogeneity of filament. Calzolaio *et al.*<sup>32</sup>

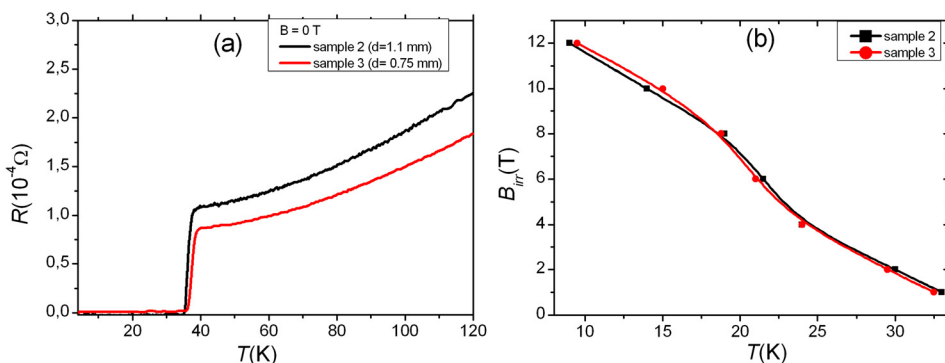


FIG. 9. (a) Resistance as function temperature in  $B = 0$  T,  $R = f(T)$ . (b) Irreversible magnetic field ( $B_{irr}$ ) as function of temperature-transport measurements,  $B = f(T)$ . The measurements were made in perpendicular magnetic field for samples 2 and 3.

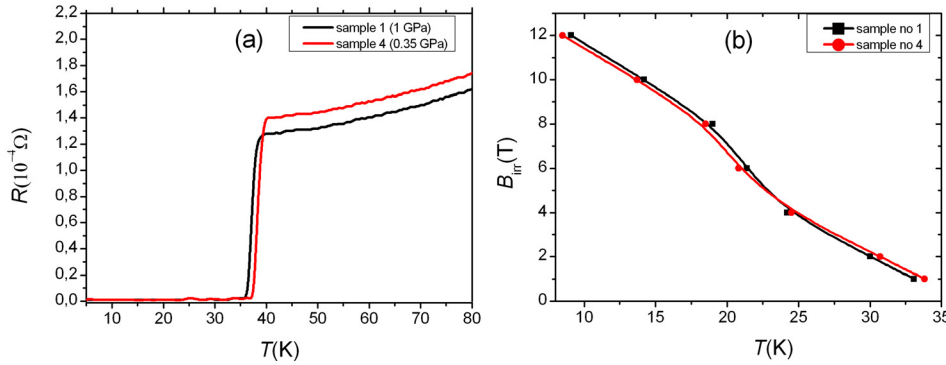


FIG. 10. (a) Resistance as function temperature in  $B = 0$  T,  $R = f(T)$ . (b) Irreversible magnetic field ( $B_{irr}$ ) as function of temperature-transport measurements,  $B = f(T)$ . The measurements were made in perpendicular magnetic field for samples 1 and 4.

showed that the  $n$  value depends on the magnetic field, temperature, and strain.<sup>32</sup> Fig. 11. shows two dependence on  $n$  value  $= f(B)$  and  $n$  value  $= f(J_c)$ . These results show that reduction of wires surface (cross section of filament) by 80% increases the  $n$  value by 50% (for  $n$  value  $= f(B)$ ). For the dependence of  $n$  value  $= f(J_c)$ , reduction of wires surface (cross section of filament) caused (e.g., for  $n$  value of 20–5 T) an significant increase of  $J_c$ .

The results in Fig. 11 are very important, because they provide a method to find the optimal application range of MgB<sub>2</sub> wires with *ex situ* MgB<sub>2</sub> barrier (the red area). We use two criteria: current density (100 A/mm<sup>2</sup>) and  $n$  value. Criterion  $n$  value is different, e.g., for NbTi in 5 T is 40–60,<sup>31</sup> for Nb<sub>3</sub>Sn in 12 T is 30–40,<sup>31</sup> and for HTSC is 15–20.<sup>31</sup> We use for undoped MgB<sub>2</sub> wire criterion proposed by Ekin.<sup>33</sup> This criterion suggests that the wires of  $n$  value larger than 20 might be used. We know that pure Mg has low resistivity in normal state. Annealing in high pressure increases melting point of Mg.<sup>4</sup> The higher melting temperature reduces the rate of synthesis reaction and can cause remains of pure Mg grains in the wire.<sup>4</sup> Moreover, Mg grains are the main influence on structure of MgB<sub>2</sub> materials, because Mg grains are three orders of magnitude larger than the B grains. These factors reduce the  $n$  value. Therefore, we consider that the criterion of Ekin is good for undoped MgB<sub>2</sub> wire with *ex situ* MgB<sub>2</sub> barrier.<sup>33</sup> Fig. 11 shows the relations of  $n = f(B)$  and  $n = f(J_c)$ . These factors are considered in the design of superconducting coils. The results in Fig. 11 show that undoped MgB<sub>2</sub> wire with an *ex situ* MgB<sub>2</sub> barrier of 0.75 mm diameter can be used in a coil, which will have maximum magnetic field of 5 T, because in this magnetic field,  $n$  value is 20 and  $J_c$  is 130 A/mm<sup>2</sup>.

#### IV. DISCUSSION OF RESULTS

The SEM results indicated that *ex situ* MgB<sub>2</sub> barrier is uniformly distributed in MgB<sub>2</sub> wires. Moreover, the results showed that the cold work increases uniformity and density of MgB<sub>2</sub> wires with *ex situ* MgB<sub>2</sub> barrier. Moreover, layers structure in sample No. 3 suggests that cold drawing increases the length of Mg grains in MgB<sub>2</sub> wires with *ex situ* barrier. The results of scanning electron microscopy showed that the pressure reduces the size of voids and grains. Moreover, this process increases the density of the MgB<sub>2</sub> material and number of connections between the grains. Our results and those of Takahashi *et al.*<sup>34</sup> show that large grains reduce the number of connections between the grains.

CD increased critical current density in pure MgB<sub>2</sub> wires, because this process reduces thickness of Mg grains and increases their length. Moreover, this process leads to an increase in the outer surfaces area of Mg grains. The larger surface of MgB<sub>2</sub> grains and 1 GPa pressure leads to more connections between grains and more pinning centers. The larger number of connections increases critical current density ( $J_c$ ) and reduces resistance after transition of superconducting material to normal state. Moreover, our results indicate that the dominant pinning mechanism on the grain boundaries (surface centers) increase  $J_c$  in the temperature range from 4.2 K to 20 K. Our results indicate that the cold drawing creates pinning centers, which poorly increase the  $J_c$  at 25 K. The strong reduction of  $J_c$  at 10 K, 20 K, and 25 K suggest that the increase of temperature strongly degrades effectiveness of surface pinning centers.

HIP of 1 GPa leads to smaller grain size, and pressure of 0.35 GPa forms bigger grain size. The grain sizes influence size and density of voids. We know that voids create point

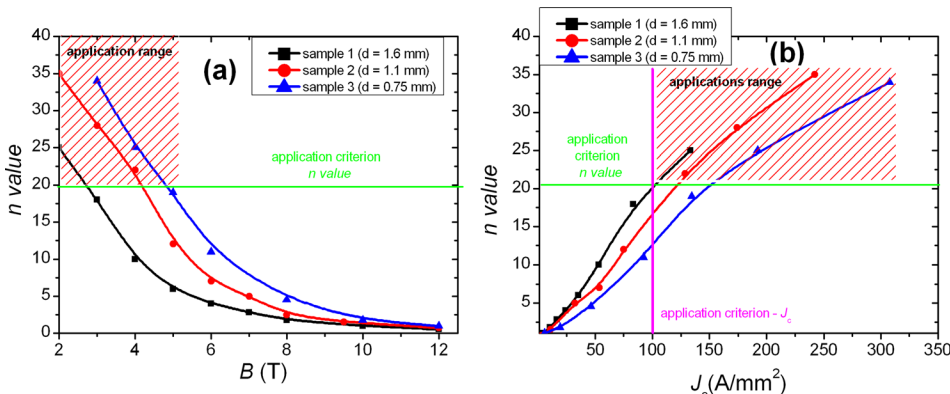


FIG. 11. (a) The magnetic fields ( $B$ ) as function of  $n$  value. (b) The critical current density ( $J_c$ ) as function of  $n$  value for undoped MgB<sub>2</sub> wires with *ex situ* MgB<sub>2</sub> barrier in perpendicular magnetic field at 4.2 K.



and surface pinning centers. These pinning centers increase  $J_c$  in low and medium magnetic fields.<sup>30</sup> Therefore, the annealing in 0.35 GPa pressure increases  $J_c$  in magnetic fields from 0 to 9 T compared to sample 1 (1 GPa), because this pressure leads to more surface and point pinning centers. 1 GPa pressure significantly reduces the size and density of voids,<sup>4</sup> and increases density of dislocation,<sup>2</sup> (line pinning centers).<sup>30</sup> High pressure and smaller grains allow for more connections between grains.<sup>2,34,35</sup> However, the results suggest that the greater number of connections between grains without pinning centers do not increase  $J_c$  in low and medium magnetic fields. Furthermore, the results for sample 1 indicate that pinning centers which increase  $J_c$  in high magnetic fields poorly increase  $J_c$  in low and medium magnetic fields. Therefore,  $J_c$  of MgB<sub>2</sub> wire annealed in 1 GPa pressure is lower in range from 0 T to 9 T than  $J_c$  of MgB<sub>2</sub> wires annealed in 0.35 GPa. The SEM results and results in articles<sup>4,28</sup> show that annealing in pressure of 0.35 GPa leads to poorer connection between the grains than that annealed in pressure of 1 GPa. These results suggest that the pinning centers affect  $J_c$  in low and medium magnetic fields more strongly than the connection between the grains.

MgB<sub>2</sub> wire made from pure Mg powder (sample 1) had higher critical current density in magnetic fields above 7.5 T than that made from MgH<sub>2</sub> powder (sample 5). On the other hand,  $J_c$  in magnetic fields below 7.5 T in wires made with pure Mg powder is lower than  $J_c$  in wires made with MgH<sub>2</sub> powder. Results of studies in article<sup>36,37</sup> show that reaction in samples 1 and 5 was the solid state of Mg and B. In this process, MgB<sub>2</sub> material exhibits smaller shrinkage by about 5%.<sup>38</sup> Increase of  $J_c$  for the sample with pure Mg is not associated with pressure (the same for both samples) and shrinking (very small by about 5%). These results suggest that impurities and voids associated with H can create surface pinning centers. These centers cause increase of  $J_c$  in the low and medium magnetic fields. Moreover, they limit the formation of line pinning centers and weaken connections between grains.

CR increases the density of the MgB<sub>2</sub> material. Annealing in samples 5 (wire) and 6 (tape) was performed in the solid state of Mg and B. Results obtained after cold rolling and annealing in pressure of 1 GPa for undoped MgB<sub>2</sub> wires with MgH<sub>2</sub> powders indicate that this process increases the density of pinning centers in low and medium magnetic fields and does not increase  $J_c$  in high magnetic fields. Shi *et al.*<sup>39</sup> indicate that the transport current flows mainly longitudinal connections. These results might suggest that cold rolling does not create line pinning centers,<sup>30</sup> at across longitudinal connection, because the cold rolling slightly increases the length of Mg grains. This process reduces thickness of the Mg grains and increase transverse surface of Mg grains. This explains why we did not observe increase of  $J_c$  in high magnetic fields and increase of  $B_{irr}$  in sample 6. Comparing  $J_c$  of wires and tapes, we can conclude that the cold drawing allows for more linear pinning centers at longitudinal connections than cold rolling. We only suppose that CR can increase the density of line pinning centers on the transverse connections. Moreover, based on results for samples 5 and 6, we can deduce that pinning centers in, e.g., SiC

doped samples in high magnetic fields can form by substitution of C for B and is not created by process of cold rolling.

In the undoped sample (No. 7) and C doped sample (No. 8) under the pressure of 0.3 GPa and annealed at the temperature of 700 °C, Mg is in liquid state and B is in the solid state.<sup>37</sup> In this process, *in situ* MgB<sub>2</sub> superconducting material shrinks by 25%.<sup>40</sup> We know that the shrinking creates stress-dislocations (line pinning centers).<sup>30,39</sup> Samples 7 and 8 were obtained in the same conditions. This indicates that the shrinking is very similar in both samples. Comparing results of samples 7 and 8, we can see that the increase of  $J_c$ ,  $F_p$ , and  $B_{irr}$  in high magnetic fields come from the substitution of C for B. In addition, the increase of  $J_c$  and  $F_p$  in medium magnetic fields comes from the point pinning centers. These centers created by C substitution on grains boundaries are of size similar to coherence length.<sup>30</sup>

Results in Fig. 9(a) show that the high pressure leads to more connectivity between the grains in the wire of 0.75 mm diameter than in the wire of 1.6 mm diameter. This indicates that pressure acts more strongly on wire of smaller diameter. Serquis *et al.*<sup>2</sup> showed that the HIP process increases the density of strain (dislocation). This result indicates that the wire of 0.75 mm diameter has more strain than the wire of 1.6 mm diameter. Greater density of strains increases the resistivity in normal state and also  $n$  value. In addition, Fig. 10(a) shows that greater density of strains decrease critical temperature.

## V. CONCLUSIONS

The HIP process leads to better control of grain size and improved density of MgB<sub>2</sub> materials. The transport results show that cold drawing and HIP increase  $J_c$  and  $F_p$  at 4.2 K, 10 K, and 20 K in undoped MgB<sub>2</sub> wires with *ex situ* MgB<sub>2</sub> barrier. These processes do not increase  $B_{irr}$  and do not decrease  $T_c$ . Cold drawing and pressure of 1 GPa also lead to significant decrease in resistance in superconducting material after the transition to normal state in wire of smaller diameter. The lower resistance indicates that wire of smaller diameter has more connections between the grains. The results for the undoped MgB<sub>2</sub> wires with *ex situ* MgB<sub>2</sub> barrier after CD and HIP show that surface pinning centers increase  $J_c$  in the range from 4.2 K to 20 K, but not at 25 K.

Calculations indicate that  $J_c$  and  $F_p$  increase in undoped MgB<sub>2</sub> wire with *ex situ* MgB<sub>2</sub> barrier after cold rolling in low and medium magnetic fields. The data for pure MgB<sub>2</sub> wires indicate that the rolling process does not increase the density of pinning centers in high magnetic fields (longitudinal connections). Moreover, the measurements show that in comparison with MgH<sub>2</sub>, the pure Mg powder increases  $J_c$  and  $F_p$  in high magnetic fields.

Analyses indicate that  $B_{irr}$  determined with the Kramer model is lower by 8% than  $B_{irr}$  determined with resistance  $R = f(T)$ . This result suggests that we can determine  $B_{irr}$  with the Kramer analysis for undoped MgB<sub>2</sub> wires with *ex situ* MgB<sub>2</sub> barrier.

$J_c$  in doped MgB<sub>2</sub> wires with *ex situ* MgB<sub>2</sub> barrier increases in high magnetic fields and decreases in low and medium magnetic fields after annealing in 1 GPa pressure. In

contrast, annealing in 0.35 GPa pressure increases  $J_c$  and  $F_p$  in low and medium magnetic fields. Our results indicate that the grains of suitable size allow for high  $J_c$  and  $F_p$  in low and medium magnetic fields, but other grains size leads to increase of  $J_c$  in high magnetic fields. Results suggest that increase of MgB<sub>2</sub> material homogeneity in wires with *ex situ* MgB<sub>2</sub> barrier can significantly reduce the anisotropy of  $J_c$ .

Annealing in high pressure of 1 GPa creates a lot of strains. These strains increase  $n$  value in undoped MgB<sub>2</sub> wires with an *ex situ* MgB<sub>2</sub> barrier.

## ACKNOWLEDGMENTS

This work was supported by the Institute of High Pressure Physics PAS and International Laboratory of HMF and LT and was also partially supported by Australian Research Council (Grant No. DE130101247) and 2014 UOW-URC Grants.

- <sup>1</sup>J. Nagamatsu, N. Nakagawa, T. Muranaka, Y. Zentani, and J. Akimitsu, *Nature* **410**, 63 (2001).
- <sup>2</sup>A. Serquis, L. Civale, D. L. Hammon, X. Z. Liao, J. Y. Coulter, Y. T. Zhu, M. Jaime, D. E. Peterson, F. M. Mueller, V. F. Nesterenko, and Y. Gu, *Appl. Phys. Lett.* **82**, 2847 (2003).
- <sup>3</sup>X. Z. Liao, A. Serquis, Y. T. Zhu, L. Civale, D. L. Hammon, D. E. Peterson, F. M. Mueller, V. F. Nesterenko, and Y. Gu, *Supercond. Sci. Technol.* **16**, 799 (2003).
- <sup>4</sup>D. Gajda, A. Morawski, A. Zaleski, T. Cetner, M. Małecka, A. Presz, M. Rindfleisch, M. Tomsic, C. J. Thong, and P. Surdacki, *Supercond. Sci. Technol.* **26**, 115002 (2013).
- <sup>5</sup>K. Adamczyk, A. Morawski, T. Cetner, A. Zaleski, D. Gajda, M. Rindfleisch, M. Tomsic, R. Diduszko, and A. Presz, *IEEE Trans. Appl. Supercond.* **22**, 6200204 (2012).
- <sup>6</sup>M. H. Hancock and N. Bay, *Supercond. Sci. Technol.* **20**, 886 (2007).
- <sup>7</sup>C. H. Jiang, H. Kumakura, and S. X. Dou, *Supercond. Sci. Technol.* **20**, 1015 (2007).
- <sup>8</sup>W. Häßler, M. Herrmann, C. Rodig, M. Schubert, K. Nenkov, and B. Holzapfel, *Supercond. Sci. Technol.* **21**, 062001 (2008).
- <sup>9</sup>D. Uchiyama, K. Mizuno, T. Akao, M. Maeda, T. Kawakami, H. Kobayashi, Y. Kubota, and K. Yasohama, *Cryogenics* **47**, 282 (2007).
- <sup>10</sup>M. A. Susner, T. W. Daniels, M. D. Sumption, M. A. Rindfleisch, C. J. Thong, and E. W. Collins, *Supercond. Sci. Technol.* **25**, 065002 (2012).
- <sup>11</sup>B. Birajdar and O. Eibl, *J. Appl. Phys.* **105**, 033903 (2009).
- <sup>12</sup>W. X. Li, R. Zeng, L. Lu, Y. Li, and S. X. Dou, *J. Appl. Phys.* **106**, 093906 (2009).
- <sup>13</sup>Z. Ma, H. Jiang, and Y. Liu, *Supercond. Sci. Technol.* **23**, 025005 (2010).
- <sup>14</sup>X. Zhang, D. Wang, Z. Gao, L. Wang, Y. Qi, Z. Zhang, Y. Ma, S. Awaji, G. Nishijima, K. Watanabe, E. Mossang, and X. Chuda, *Supercond. Sci. Technol.* **23**, 025024 (2010).
- <sup>15</sup>M. S. A. Hossain, C. Senatore, R. Flukiger, M. A. Rindfleisch, M. J. Tomsic, J. H. Kim, and S. X. Dou, *Supercond. Sci. Technol.* **22**, 095004 (2009).
- <sup>16</sup>M. S. A. Hossain, C. Senatore, M. Rindfleisch, and R. Flukiger, *Supercond. Sci. Technol.* **24**, 075013 (2011).
- <sup>17</sup>M. Kulich, R. L. Flukiger, C. Senatore, M. Tropeano, and R. Piccardo, *Supercond. Sci. Technol.* **26**, 105019 (2013).
- <sup>18</sup>K. Togano, J. M. Hur, A. Matsumoto, and H. Kumakura, *Supercond. Sci. Technol.* **22**, 015003 (2009).
- <sup>19</sup>E. Martinez, L. A. Angurel, S. I. Schlachter, and P. Kovac, *Supercond. Sci. Technol.* **22**, 015014 (2009).
- <sup>20</sup>M. Wozniak, K. L. Juda, S. C. Hopkins, D. Gajda, and B. A. Glowacki, *Supercond. Sci. Technol.* **26**, 105008 (2013).
- <sup>21</sup>R. Zeng, L. Lu, W. X. Li, J. L. Wang, D. Q. Shi, J. Horvat, S. X. Dou, M. Bhatia, M. Sumption, E. W. Collings, J. M. Yoo, M. Tomsic, and M. Rindfleisch, *J. Appl. Phys.* **103**, 083911 (2008).
- <sup>22</sup>J. H. Kim, S. X. Dou, D. Q. Shi, M. Rindfleisch, and M. Tomsic, *Supercond. Sci. Technol.* **20**, 1026 (2007).
- <sup>23</sup>A. Morawski *et al.* "Composite electric conductors and method for their manufacture," UK patent No. 0,706,919.8, U.S. patent No. 60/907,590, available at: <http://www.wipo.int/pctdb/en/index.jsp>.
- <sup>24</sup>A. Kario, A. Morawski, W. Häßler, M. Herrmann, C. Rodig, M. Schubert, K. Nenkov, B. Holzapfel, L. Schultz, B. A. Glowacki, and S. C. Hopkins, *Supercond. Sci. Technol.* **23**, 025018 (2010).
- <sup>25</sup>A. Kario, A. Morawski, B. A. Glowacki, T. Lada, M. Smaga, R. Diduszko, D. Kolesnikov, A. J. Zaleski, A. Kondrat, and D. Gajda, *Acta Physica Polonica A* **111**(5), 693–703 (2007).
- <sup>26</sup>D. Gajda, A. J. Zaleski, A. Morawski, and A. Karia, *Acta Physica Polonica A* **113**(1), 371–374 (2008).
- <sup>27</sup>A. Morawski, T. Łada, and K. Przybylski, *Physica C* **387**, 143–147 (2003).
- <sup>28</sup>T. Cetner, A. Morawski, M. Rindfleisch, M. Tomsic, A. Presz, D. Gajda, A. Zaleski, and O. Tachenko, *ICMC 2010 Proceedings* (Wrocław University of Technology Publishing House, Wrocław, 2011), pp. 1237–1241.
- <sup>29</sup>Z. X. Shi, M. A. Susner, M. Majoros, M. D. Sumption, X. Peng, M. Rindfleisch, M. J. Tomsic, and E. W. Collins, *Supercond. Sci. Technol.* **23**, 045018 (2010).
- <sup>30</sup>J. D. Livingston, GE R&D Center Report (1969–1970), available at [www.bnl.gov/magnets/staff/gupta/Summer1968/0377.pdf](http://www.bnl.gov/magnets/staff/gupta/Summer1968/0377.pdf).
- <sup>31</sup>A. K. Ghosh, *Physica C* **401**, 15–21 (2004).
- <sup>32</sup>C. Calzolaio, P. Bruzzone, and F. Roth, *Supercond. Sci. Technol.* **26**, 075024 (2013).
- <sup>33</sup>J. W. Ekin, *Experimental Techniques for Low-Temperature Measurements* (Oxford University Press, 2006).
- <sup>34</sup>M. Takahashi, M. Okada, T. Nakane, and H. Kumakura, *Supercond. Sci. Technol.* **22**, 125017 (2009).
- <sup>35</sup>X. Xu, J. H. Kim, M. S. Hossain, J. S. Park, Y. Zhao, and S. X. Dou, *J. Appl. Phys.* **103**, 023912 (2008).
- <sup>36</sup>D. Gajda, A. Morawski, A. Zaleski, M. Kurnatowska, T. Cetner, G. Gajda, A. Presz, M. Rindfleisch, and M. Tomsic, *Supercond. Sci. Technol.* **28**, 015002 (2015).
- <sup>37</sup>J. L. Pelissier, *Phys. Scr.* **34**, 838 (1986).
- <sup>38</sup>M. M. Avedesian and H. Baker, *ASM Specialty Handbook: Magnesium and Magnesium Alloys* (ASM International, Materials Park, OH, 1999).
- <sup>39</sup>Z. X. Shi, M. A. Susner, M. D. Sumption, E. W. Collins, X. Peng, M. Rindfleisch, and M. Tomsic, *Supercond. Sci. Technol.* **24**, 065015 (2011).
- <sup>40</sup>A. Jung, S. I. Schlachter, B. Runtzsch, B. Ringsdorf, H. Fillinger, H. Orschulko, A. Drechsler, and W. Goldacker, *Supercond. Sci. Technol.* **23**, 095006 (2010).